Published in final edited form as:
Nanomedicine. 2014 January ; 10(1): . doi:10.1016/j.nano.2013.06.010.

In Vivo Human Time-Exposure Study of Orally Dosed Commercial Silver Nanoparticles

Mark A. Munger, Pharm.D.[*,†], **Przemyslaw Radwanski, Pharm.D., Ph.D.**[‡], **Greg C. Hadlock, Ph.D.**[‡], **Greg Stoddard, M.S.**[†], **Akram Shaaban, M.D.**[¶], **Jonathan Falconer**[§], **David W. Grainger, Ph.D.**[§], and **Cassandra E. Deering-Rice, Ph.D.**[‡]

[*]Department of Pharmacotherapy University of Utah, Salt Lake City, Utah 84112 USA

[‡]Department of Pharmacology and Toxicology University of Utah, Salt Lake City, Utah 84112 USA

[§]Department of Pharmaceutics and Pharmaceutical Chemistry University of Utah, Salt Lake City, Utah 84112 USA

[†]Department of Internal Medicine University of Utah, Salt Lake City, Utah 84112 USA

[¶]Department of Radiology University of Utah, Salt Lake City, Utah 84112 USA

Abstract

Background—Human biodistribution, bioprocessing and possible toxicity of nanoscale silver receives increasing health assessment.

Methods—We prospectively studied commercial 10- and 32-ppm nanoscale silver particle solutions in a single-blind, controlled, cross-over, intent-to-treat, design. Healthy subjects (n=60) underwent metabolic, blood counts, urinalysis, sputum induction, and chest and abdomen magnetic resonance imaging. Silver serum and urine content was determined.

Results—No clinically important changes in metabolic, hematologic, or urinalysis measures were identified. No morphological changes were detected in the lungs, heart or abdominal organs. No significant changes were noted in pulmonary reactive oxygen species or pro-inflammatory cytokine generation.

Conclusion—*In vivo* oral exposure to these commercial nanoscale silver particle solutions does not prompt clinically important changes in human metabolic, hematologic, urine, physical findings or imaging morphology. Further study of increasing time exposure and dosing of silver nanoparticulate silver, and observation of additional organ systems is warranted to assert human toxicity thresholds.

Corresponding Author Mark A. Munger, Pharm.D. University of Utah 30 South, 2000 East, Rm #201 Salt Lake City, Utah 84112-5820 USA Phone: +1 (801) 581-6165 Fax: +1 (801) 585-7316 mmunger@hsc.utah.edu.

Conflict of Interest: The authors declare no conflicts of interest or financial interests in any product or service mentioned in this article, including grants, employment, gifts, stock holdings, honoraria, consultancies, expert testimony, patents, and royalties.

Trial Registration: Clinical-Trials.gov: https://register.clinicaltrials.gov/ (Identifier: NCT01243320 and NCT01405794).

Keywords

biological activity – nanoparticles; nanotechnology; nanotoxicology – oral ingestion; safety research

Introduction

Nanotechnology is driving potentially the most important engineering revolution since the industrial age. Currently, over 1,300 manufactured nanotechnology-enabled consumer products are available in the marketplace.[1] This abundant, increasingly common consumer accessibility to engineered nanomaterials included in diverse health, cosmetic, food and agricultural, recreational equipment and clothing products has afforded increasing exposure of human tissue and physiology to different routes of nanomaterial entry into the human body. The consequences of such exposure, both deliberate and inadvertent, to large populations are currently debated, with little current consensus on the risks, toxicities, risk management and exposure.[2-5] This scenario has contributed to nanoparticulate silver's reemergence as a nutraceutical product and possible medical modality.[6-8] Nanoscale silver makes up approximately a quarter of the inventory of the present commercially available nanoproduct inventory. With centuries of silver therapeutic attributes, silver nanoproducts are claimed to provide unique physiochemical properities and biological activities broadening its application as an antibacterial, anti-viral, and anti-inflammatory therapy.[9-12] However, elemental silver in nanoparticulate form (i.e., Ag^0) has distinct physical, chemical and toxicological properities from long-studied soluble silver ions (Ag^+_{aq}) made bioavailable from diverse salts. Increasing systemic exposure to humans in dermally absorbed, opthalmologically applied, ingested, inhaled and possibly parenterally injected silver forms facilitates vascular transport and penetration of silver nanoparticles across tissue surfaces and through membranes. Human bioavailability, biodistribution, and possible accumulation of these nanoparticles have not been reported. Therefore, the potential for evasion of immune cell-based clearance, leading to systemic acute or chronic cytotoxicity or illness remains an open question.[8]

A growing body of in vitro evidence supports cell toxicity for silver nanoparticles in concentrations between 5-50 μg/ml. The lung,[12-14] liver,[10,15-18] brain,[19] vascular system,[20] and reproductive systems[21-22] may be negatively influenced. Given the increased introduction of engineered new nanoscale products into the consumer marketplace, it is important to understand whether *in vitro* findings translate to *in vivo* human toxicity.

To this end, we studied in an intent-to-treat analysis 60 healthy volunteers through several time-length exposures to orally dosed commercial silver nanoparticles in a prospective, placebo-controlled, single-blind, dose-monitored, cross-over design. The study is the first to quantitate changes in human metabolic, hemotologic, and sputum morphology, and to monitor for changes in physical findings and organ imaging after exposure to a commercially available aqueous silver colloid nanoparticle oral formulation.

Methods

Study Population

Two intent-to-treat studies were conducted at the University of Utah Lung Health Study Clinic and Center for Clinical and Translational Sciences at the University of Utah Hospital. Each subject underwent a screening evaluation to assess enrollment eligibility. Sixty healthy volunteers, between 18-80 years of age, were subsequently enrolled (i.e., 10 ppm oral silver particle dosing [36 subjects] and 32 ppm oral silver particle dosing [24 subjects]). Females

of child-bearing potential, defined as women physically capable of becoming pregnant, whose career, lifestyle, or sexual orientation precluded intercourse with a male partner and women whose partners were using 2 barrier birth control methods or hormonal contraceptive method were allowed to participate. Subjects with a history of any heavy metal allergy; asthma, chronic bronchitis or emphysema; or renal impairment defined by a creatinine clearance ≤ 30 ml/minute; or significant acute or chronic disease as determined by the investigators were excluded. Subjects unable to complete the study were excluded from analysis and replaced.

All patients provided written informed consent. The study was conducted in accordance with the International Conference on Harmonisation of Technical Requirements for Registration of Pharmaceuticals for Human Use Guidelines for Good Clinical Practice and the Declaration of Helsinki, and received approval from the University of Utah Institutional Review Board. The trials are registered with Clinical-Trials.gov (Identifier: NCT01243320 and NCT01405794).

To minimize risk to study subjects, a dose-time escalation dosing scheme was employed. Study one used 10 ppm oral silver particle dosing with 3-, 7-, and 14-day time periods; study two used 32 ppm for 14 days. After completion of each time period, an independent Data Safety and Monitoring Board (DSMB) reviewed every measurement for evidence of toxicity.

Study Product

The silver nanoparticle (AgNP) study product was manufactured by American Silver, LLC. (Alpine, Utah, USA) by a published AC high voltage (10(3)-10(4)) aqueous electrolysis of de-ionized water using silver metallic electrodes as detailed previously (US patents 6,214,299 and 7,135,195).[7,23] Silver is in the form of zero-valent elemental silver particles coated with silver oxide, with manufacturer's claims to particle size ranging between 5-10 nm (10 ppm; lot #122810) or claims to a mean of 32.8nm, range of 25-40 nm (32 ppm: lot #071511), respectively. The average daily ingestion of this elemental silver colloid formulation is estimated to be 100 μg/day for 10 ppm, and 480 μg/day for 32 ppm silver.

Silver nanoparticle characterization

Silver particle sizing—To determine nanoparticle hydrodynamic diameter, dynamic light scattering (DLS) was performed on the 32 ppm AgNPs (lot #09280, 32 ppm silver) in Millipore ASTM grade I water using a commercial instrument (Brookhaven Instruments, Holtsville, USA) at a laser wavelength of 677nm and fixed angle of 90° at 25°C after instrument calibration using 100-nm diameter commercial polystyrene nanosphere size standards (Thermo Scientific, Fremont, California, USA). Instrument background was tested with a control sample of 0.2 micron filtered Millipore American Society for Testing and Materials (ASTM) grade I prior to sampling and no sub-micron particles were detected. Cuvette temperature was controlled using a recirculation bath. Optical scattering intensities were collected at 50% laser intensity to ensure proper particle counts. Each measurement was taken between 5 and 10 minutes' duration. Time correlation functions of scattered intensity were calculated by inverse Laplace transformation (regularized positive exponent sum) as described previously. Optical spectroscopy and plasmon absorption analysis were performed on the 32 ppm silver nanoparticles using a Varian Cary 400 Bio Ultraviolet (UV)–visible spectrophotometer (Varian Cary, Palo Alto, California). Two 1-cm quartz cells were used: one cell containing sample and one reference cell containing ASTM grade I water. Scans were performed at 5nm per second from 800 to 200 nm. Samples were vortexed prior to measurement at ambient temperature.

Silver ion content—The study silver solution (lot #09280, 32 ppm) was centrifuged for 120 minutes at 20,800 RCF x g, separating >96% of silver nanoparticles >10 nm in diameter to obtain a supernatant with residual ions.[25] Inductively coupled plasma mass spectrometry (ICP-MS) was then performed on the supernatant using a liquid chromatographyICP-MS (LC-ICP-MS) Agilent 7500ce (Agilent Technologies, Inc., Santa Clara, California USA). Fresh silver ion standards were prepared prior to sample analysis using known concentrations (0.028-0.833 ppm) of silver nitrate ($AgNO_3$) (Inorganic Ventures, Christiansburg, Virginia USA) in ASTM grade I (Millipore filtered) ultrapure water. All ICP-MS samples (centrifuged supernatants or uncentrifuged product stock) were oxidized with nitric acid to solubilize residual silver nanoparticles to ions. Aliquots of each supernatant or product sample were measured in triplicate. Detection limit for silver ion in this instrument was determined to be 0.1 ppb using the standards.

Study Design for Metabolic Panel, Silver Concentrations, Induced Sputum, and MRI

Subjects received silver nanoparticle colloidal solution diluent (e.g. sterile water [no silver nanoparticles]) followed by the active silver solution). A 72-hour washout period preceded the dosing cross-over. Each subject received 15 mL of study material daily from a pre-mixed oral syringe. Each dose administration was observed by study personnel to ensure compliance. Subjects were blinded to the study product received.

At baseline and the end of each time-period, subjects underwent a medical and drug history, complete physical examination, comprehensive metabolic panel, blood count with differential and urinalysis. Blood and urine were collected for serum and urine silver concentrations at trough concentrations (≥24 hours post-dose) for the 3- and 7-day time periods at 10 ppm and at peak concentration (≤ 2 hours post-dose) for the 14-day 10 ppm dose and for the 32 ppm study population. Silver concentrations in serum and urine were determined by using ICP-MS (NMS Laboratories, Willow Grove, USA). Calibration silver samples in dilute nitric acid and controls in human serum matrix were used in each ICP-MS assay cohort. The ICP-MS assay dynamic range of silver samples for this study were 0-40 μg/L. Sputum was collected by induction protocol within 24 hours of the last dose for each time-period, as previously described.[26]

Sputum Analysis

Hydrogen peroxide concentrations were determined using a modification of a previous method.[27] Peroxiredoxin protein expression was measured as described.[28] Determination of RNA expression using quantitative real-time polymerase chain reaction (qPCR) was determined by methods previously described.[29]

Magnetic Resonance Imaging (MRI) Protocols

A cardiac and abdominal MRI was obtained at the end of each phase of each time period. Patients were examined on a 1.5-T 32-channel superconducting magnetic resonance system (Magnetom Avanto, Siemens Medical Solutions). Cardiac MRI studies were performed using breath-hold acquisitions prospectively triggered by the electrocardiogram. Cine steady-state free precession (SSFP) and true fast imagning magnetic resonance with steady state precession (TrueFISP) cardiac images were acquired in multiple standard short-axis and long-axis views, including specific right ventricular outflow tract (RVOT) and left ventricular outflow tract (LVOT) orientations (slice thickness 8 mm, echo time 1.2 ms, pixel bandwidth 1.150 hertz (Hz), repetition time 3.0 ms, temporal resolution about 43 ms, matrix 256 × 202). Abdominal MRI protocol included a transverse T1-weighted fast gradient-recalled dual-echo sequence (TR/in-phase TE/out-of-phase TE, 129/4.36/2.0; flip angle, 70°; matrix, 134 × 256; section thickness and intersection gap, 6 and 0.6 mm; signal average, 1; field of view, 220–340 mm [depending on body habitus]) and a transverse T2-weighted Half

Fourier Acquisition Single Shot Turbo Spin Echo (HASTE) (time to repetition (TR)/echo time (TE), 1,000/89; refocusing angle, 180°; slices, 20; slice thickness, 6 mm with a 10% gap; matrix, 168–192 × 256; field of view, 220–340 mm [depending on body habitus]). A dynamic contrast-enhanced 3 dimensional (D) gradient-echo volumetric interpolated breath-hold examination (VIBE) sequence was performed in the arterial, venous, and delayed phases, after the injection of 0.1 mmol/kg of body weight of Gadopentetate dimeglumine (Magnevist; Bayer HealthCare Pharmaceuticals, Berlin, Germany) at a rate of 2 mL/s using a pressure injector. This was followed by delayed contrast-enhanced cardiac study using a segmented inversion–recovery sequence in the same views used for cine cardiac MRI 10–20 min after contrast administration. All images were deidentified and transferred to a 3D postprocessing workstation (Leonardo, Siemens Healthcare). LV function and volumes were calculated by planimetry of the endocardial and epicardial borders from the serial short-axis views (usually 8–14) with no gap between the slices. Ejection fraction, end diastolic volume and end systolic volume were analyzed.

Statistical Analysis

Average effect analysis was employed to assess toxicity. A ±4 SD range was applied as the statistical rule based on the concept that a normal distribution contains nearly all individual observations within a ±3 SD interval. A mixed effects linear regression model with repeated measurements from the crossover periods nested within subjects was used to determine effect differences. In this model, the baseline value was included as a covariate. The crossover period was the primary predictor variable. To test for a linear trend across exposure time, the 3-, 7-, and 14-days a mixed effects model using exposure time as the predictor was fitted. The *p* value for the time variable in such a model represents a linear dose-response significance test. All reported *p* values were from a two-sided comparison.

The power of the study to detect toxicity was sufficient for individual observation analysis and the usual mean difference analysis. Combining the 10 ppm and 32 ppm silver colloidal solutions, for a total sample size of n=60, based on a binomial probability, using 1-Prob(observed incidence=0|true incidence=0.027), the total sample size of n=60 provided 80% probability of observing toxicity in at least one study subject if the true toxicity incidence is 2.7%. For the analysis examining paired sample mean differences between placebo (diluent only) and active silver solution, the n=24 subjects with maximum exposure of 32 ppm silver colloidal solution for 14 days provided 80% power to detect a mean difference of 0.48 standard deviations (SD), using a two-sided alpha 0.05 comparison and assuming a correlation of r=0.70 between the placebo and active phases. Given a reference range is ±2SDs, the effect sizes of 0.48SD and 0.30SD represented detectable effects well within normal laboratory reference ranges.

Results

A total of 62 subjects were enrolled in the study. Sixty subjects completed the study. Two were discontinued, one due to inability to draw blood (subject never received study product) and one due to hospitalization for pulmonary embolism (subject received 12 days of placebo diluent only). (Table 1)

Silver nanoparticles used here were commercially prepared by alternating current high voltage (10^3 volts) aqueous electrolysis of silver salt solutions as detailed previously.[7,23] These previous studies on the same particles of 32ppm product showed that the process produces nanoparticles 20-40nm in diameter, with the dominant crystalline solid phase being metallic silver as asserted by scanning electron microscope, transmission electron microscope, Raman and UV/Visible spectrometry analysis.[7,23] The metallic nanoparticle silver has some oxygen, proposed as an oxide or ‘oxyhydroxide’ overlayer in the sol,

consistent with minute amounts of crystalline silver oxide under TEM studies.[7,23] Many 20–30 nanometer (nm) silver nanoparticles comprise a substructure, with 5–7 nm particles held together by relatively weak bonds.[7,23]

Optical spectroscopic analysis of silver nanoparticles

The visible appearance of the as-supplied commercial silver solution from the stock bottle was yellow, consistent with the presence of typical silver nanoparticles with plasmon behavior.[30] Optical absorption of silver colloids (see Figure 1) also supports the presence of silver nanoparticles. The molar extinction coefficient for silver particles is considerable ($3\times10^{11}M^{-1}cm^{-1}$), providing a strong, distinct absorption band at low concentrations. The peak and width of the spectrum in Figure 1 follow theoretical Mie optical plasmon predictions consistent with previously reported results for similar silver nanoparticle systems.[31] Full width at half maximum absorbance was found to be 150 nm and λ_{max} was determined to be 448 nm. Although the observed peak position of the surface plasmon band is slightly larger than these previously reported, its position is still consistent with Mie theory predictions. This optical absorption strongly depends on particle size, extent of aggregation,[32] dielectric, and chemical properties of the milieu.[33] Small silver spherical nanoparticles (i.e., <20nm diameter) exhibit a single, narrow surface plasmon band inconsistent with experimental observations here.[34] Previous data suggested that for a full width at half maximum (FWHM) of 229 and a λ_{max} of 400 nm, silver nanoparticle size was determined to be 63 ± 19 nm.[35] Direct size predictions from particle optical absorption are difficult because of many influences on the system, but the red-shifting of the surface plasmon absorption band maximum to 448nm and FWHM bandwidth broadening both indicate some alteration of ideal plasmonics compared to theoretical predictions calculated for silver nanoparticles.[36] Specifically, the spectrum supports a broad polydispersity of these commercial silver nanoparticles, prepared in water by high voltage electrolysis.[7,23] This method also seems to produce particles that experience aggregation or size dispersity to produce the spectral shift and broadening observed.[36] Previous data provide evidence that exposure of silver nanoparticles to low-level UV light (including ambient laboratory lighting) can convert spherical AgNPs to nanoprisms with a corresponding red-shift in their UV absorbance profile.[37] However, the silver nanoparticles are shipped and stored from the commercial supplier in light-protected (opaque) plastic stock bottles in DI water and transferred to sterile, but transparent plastic dispensing syringes in the clinical trials dispensing room prior to each patient's oral dosing/administration. Light effects changing silver particle sizes are therefore considered unlikely. Finally, the observed spectrum minimum at ~320nm corresponds to the wavelength at which both real and imaginary parts of the silver particle's dielectric function diminish drastically, consistent with other similar observations for silver NP systems.[34] Hence, the collective UV/Vis optical data support the presence of silver NPs with broad sizing polydispersity and classic plasmonic properties of particles with sizes below 100nm.

Silver nanoparticle DLS hydrodynamic diameter determinations

Figure 2 shows that the average silver nanoparticle hydrodynamic diameter was determined by dynamic light scattering (DLS) to be 59.8 nm ± 20 nm. This particle size is consistent with that expected for the observed absorption maximum of λ_{max}~448 nm from Figure 1, given the broad particle polydispersity.

Silver ion content

ICP-MS detected quantitative recovery of total silver from the (as supplied) nitric acid-digested 32ppm product stock sample (average control silver content of 31.5 ± 0.2 ppm). Importantly, significant amounts of silver ion were recovered in the supernatant of all centrifuged samples analyzed (26.8 +/− 0.6 ppm silver ion), corresponding to ionic silver

comprising some 84.3% of the total silver content in the product administered orally to patients.

Clinical Findings

For all outcomes measured in the subjects administered the 10 ppm dose at 3-, 7-, and 14-day day exposure, a linear trend across exposure times was tested in a mixed effects model without a significant trend in any outcome (all $p<0.20$). Thus, combining the various exposure groups into the one large, a 10 ppm group, provided greater statistical power for the 10 ppm versus 32 ppm dose comparisons. Changes in subject hemodynamics are listed in Table 2. No clinically important changes in weight, BMI, systolic or diastolic blood pressure or heart rate were noted. However, heart rate significantly declined by 2.3 beats per minute for the total group.

Results of the complete metabolic panel are listed in Table 3. There were no significant or clinically important changes observed in laboratory finding across the total population. Blood urea nitrogen and alanine aminotransferase tests from the 10 ppm dose were analyzed to be statistically significant, but nothing in the 32 ppm dose cohort was noted. However, when the 95% CI limits of these significant tests are added to the mean value of the active period, representing a statistical comparison to the normal reference range limits, all values remain within the normal reference range. There was no significance in any metabolic test, suggesting that increasing dosing from 10 to 32 ppm does not elicit silver toxicity. The results of the complete blood count with differential are displayed in Table 3. Comparison of the red blood cell count (RBC) between active vs. placebo solutions was significant at the 10 ppm dose, but not at the 32 ppm dose. There were no clinically important changes in any blood count value including erythrocytes, granulocytes, or agranulocyte counts. Exposure time was not associated with changes in blood counts.

No significant or clinically important changes were evident in the complete urinalysis. Although there were individual subject positive tests for urine ions, proteins, blood cells, and some other solutes, these changes remained unchanged in comparison between the active and placebo solutions.

Serum Silver and Urine Findings

Serum and urine silver concentrations were determined at different time variables. There was no detection of serum silver from subjects at trough concentrations throughout the 3- and 7-day time periods at 10 ppm. Peak serum silver concentration was detected in 42% of subjects in the 14-day 10 ppm dosing showing a mean of 1.6±0.4 mcg/L. The 32 ppm dose mean concentration was detected in 92% of subjects at 6.8±4.5 mcg/L. No silver was detected in the urine, independent of dose or time period.

Sputum Reactive Oxygen Species (Hydrogen Peroxide) and Pro-Inflammatory Cytokine RNA Findings

Quality paired samples allowing determination of ROS concentrations and pro-inflammatory cytokine RNA expression were analyzed in 72% and 83% of 10 ppm and 32 ppm study samples, respectively (Table 4). No statistically significant change in markers of hydrogen peroxide production or peroxiredoxin protein expression were detected. Analysis of IL-8, IL-1α, IL-1β, MCP1 and NQO1 also showed no statistical difference between the active silver and placebo solutions.

MRI Findings

Eighteen 10 ppm and eleven 32 ppm subjects underwent a post 3-14 day, respective active and placebo solution cardiac and abdominal MRIs. No morphological or structural changes were noted between active and placebo solutions.

Discussion

Nanoscale colloidal elemental silver is widely found in diverse consumer products, medical devices, and pharmaceuticals.[1] Therefore, study of human processing and possible toxicological response to this nanomaterial is critically important to understanding potential human exposure risks and benefits. To assess the human risk of oral ingested exposure to a commercial nanoscale silver product, we conducted a prospective, controlled, parallel design systematic *in vivo* study with two doses of a commercial silver nano-particle solution over a 3-14 day monitored exposure. Findings show that this colloidal elemental silver particulate formulation produces detectable silver (presumed to be $Ag^{+}_{(aq)}$ ion) in human serum but do not demonstrate clinically significant changes in metabolic, hematologic, urine, physical findings, sputum morphology or imaging changes. To our knowledge, this is the first systematic *in vivo* human study of a systemic ingested nanoscale product.

Oral administration of the silver aqueous product delivers both ionic silver and silver nanoparticles. Given the substantial fraction of ionic silver in the product detected by ICP-MS, and very limited GI absorption of metallic nanoparticles of similar size in other studies in rodents, we assert that most silver detected in patient blood samples is ionic, with no evidence that intact silver nanoparticles are either absorbed into circulation through the human digestive tract, or attached to blood components (e.g., proteins, platelets and cells).[38]

Recent reports detail the potential for human toxicity from nanoparticles of various natural and engineered forms, material chemistries and morphologies, and exposure routes. Suggested and defined target organ systems susceptible to nanoparticle adverse health effects include the pulmonary, cardiovascular, neurologic, reticuloendotheilal, renal, and reproductive systems.[5,39-41] To this end, the literature has called for new toxicological study designs to establish procedures capable of reliable predictive assay of nanoparticles in model *in vitro* systems, as well as the critical need for validating *in vivo* studies.[5,42-43] Our study begins to address existent human toxicity to silver oral nanoparticle exposure in a systematic way.

Abdominal organ system toxicity has been shown to occur from exposure to silver nanoparticles. The liver, in particular, has been noted as a toxicity target, possibly due to oxidative stress.[15] Non-cytotoxic doses of silver nanoparticles reduced cell mitochondrial function, cell profileration, and induced apoptosis in rat and human liver, and human mesenchymal cell lines *in vitro*, respectively.[15-16,] We have shown in MDR1.C and Hep G2 cell lines that after 24 hour exposure of a commercial 32 ppm silver nanoparticle solution where cell viability was maintained that nanoscale colloidal silver may be a potential source of drug-drug interactions.[45] Potential interactions may occur through reductions in NADPH cytochrome c reductase activity.[46] In contrast, a prospective, controlled 90-day exposure of 56 nm silver nanoparticles at 30 mg/kg *in vivo* in rats did not show any clinical chemistry, hematological, body weight, food consumption, or water intake changes.[47] Our human clinical findings correlate closely with these results. Hence, potential *in vitro* hepatocellular toxicity could occur from non-cytotoxic doses of nanoscale silver but these results do not correlate with *in vivo* rat or our human findings. Reasons for this disconnect, while often observed in nanomaterials toxicity exposure studies, may result from differences using *in vitro* direct nanoparticle-cell exposure, non-comparable dosing to cultured cells versus *in vivo* systemic exposure, or incomplete understanding of nanoscale silver particle *in vivo*

bioavailability, biodistribution, or liver blood flow dynamics and processing. MRI results from this study were not able to differentiate any abdominal changes from exposure to nanoscale silver.

The lung is another major target of silver nanoparticle exposure, particularly through inhalation. Silver nanoparticles (15-18 nm) may bind to lung epithelial cells and alveolar macrophages, producing reactive oxygen species, potentially limiting function of cells[10, 12, 13, 47] Histopathological examination from inhaled 18 nm silver nanoparticles for 90 days in Sprague-Dawley rats shows dose-dependent alveolar infiltration, thickened alveolar walls and small granulomatous lesions.[13] These histology changes were associated with reductions in tidal and minute volumes. Intratracheally instilled silver nanopowders enhanced systemic platelet aggregation in rats.[48] Silver nanoparticles enhance thrombus formation through increased platelet aggregation and procoagulant activity.[49] Congruence of results from multiple *in vitro* and a single *in vivo* animal models support cellular and functional toxicity from inhaled nanoscale silver particles. However, orally dosed nanoscale silver from our study failed to induce detectable changes in reactive oxygen species or pro-inflammatory cytokine RNA from induced sputum samples. This attributed to poor absorption of silver nanoparticles in the gut and poor translocation of these particles to the respiratory system from the gastrointestinal route.[38, 49]

Further studies are necessary to better understand possible silver nanoscale particle toxicity risks on the human reproductive system, systemic bioavailability and toxicity from subcutaneous delivery systems or from leaching of embedded silver in catheter-based medical devices, and to the central nervous system from different delivery systems. Our limited study did not assess these other physiologic systems or other delivery systems. Our study timeframe of 14 days, although one dosing interval, should be extended to better determine whether longer particle oral exposure leads to higher silver systemic bioavailability and subsequent accumulation in human lipid compartments, a possible source of chronic toxicity. Another important issue regards the form of silver detected in serum in the patients in this study: ICP-MS detects silver in ionic form, and our analytical methods cannot discriminate ionic silver from nanoparticulate silver in physiological fluids. However, the ICP-MS product analysis indicates that oral administration of the silver aqueous product delivers both ionic silver and silver nanoparticles to humans. Given the substantial fraction of ionic silver ($Ag^{+}_{(aq)}$) resident in the as-supplied product as detected by ICP-MS, and very limited GI absorption of metallic nanoparticles of similar size in other studies in rodents[38] we assert that most silver detected in patient blood samples is ionic, with no evidence that intact silver nanoparticles are either absorbed into circulation through the human digestive tract, or attached to blood components (e.g., proteins, platelets and cells). Previous studies on nanoparticle colloidal gold oral bioavailability showed that miniscule (<1%) amounts of 10-nm gold nanoparticles permeate across the gut to enter systemic vascular circulation from the intestine in rodents.[51] We assert that silver metallic particle absorption is similar, and that the silver detected in serum in human subjects is first solubilized from ingested colloidal form in the upper gastrointestinal tract and absorbed into blood in ionic form.

In summary, nanoscale colloidal silver is an increasingly deployed engineered nanomaterial, with potential nutraceutical and therapeutic properties, increasingly found in consumer products and medical devices. We have demonstrated that 14-day monitored human oral dosing of a commercial oral nanoparticle silver colloidal product does not produce observable clinically important toxicity markers. Further study of nanomaterials over longer human exposures is clearly warranted to determine risks.

Acknowledgments

The authors express appreciation to The Utah Lung Health Study Clinic, and Nicholas Cox, and Angela Wolsey for their technical and clinical support.

Funding: This study was funded in part by Award Number UL1RR025764 from the National Center for Research Resources.

References

1. The Project on Emerging Nanotechnologies. [Accessed: 01/12/2012] Nanotech-enabled Consumer Products Continue to Rise. http://www.nanotechproject.org/news/archive/9231/
2. Grainger DW. Nanotoxicity assessment: all small talk? Adv Drug Deliv Rev. 2009; 61(6):419–21. [PubMed: 19386273]
3. Oberdörster G. Safety assessment for nanotechnology and nanomedicine: concepts of nanotoxicology. J Intern Med. 2010; 267(1):89–105. [PubMed: 20059646]
4. Becker H, Herzberg F, Schulte A, Kolassa-Gehring M. The carcinogenic potential of nanoparticles, their release from products and options for regulating them. Int J Hyg Environ Health. 2011; 214(3): 231–8. [PubMed: 21168363]
5. Johnston HJ, Hutchison G, Christensen FM, Peters S, Hankin S, Stone V. A review of the in vivo and in vitro toxicity of silver and gold particulates: Particle attributes and biological mechanisms responsible for the observed toxicity. Crit Rev Toxicol. 2010; 40(4):328–46. [PubMed: 20128631]
6. Samberg ME, Orndorff PE, Monteiro-Riviere N. Antibacterial efficacy of silver nanoparticles of different sizes, surface conditions and synthesis methods. Nanotoxicol. 2011; 5(2):244–53.
7. Roy R, Hoover MR, Bhalla AS, Slawecki T, Dey S, Cao W, et al. Ultradilute Ag-aquasols with extraordinary bacteriocidal properties: Role of the system Ag-0-$H_2$0. Mat Resear Innovat. 2007; 11:3–18.
8. Atiyeh BS, Costagliola M, Hayek SN, Dibbo SA. Effect of silver on burn wound infection control and healing; review of the literature. Burns. 2007; 33:139–48. [PubMed: 17137719]
9. Elechiguerra JL, Burt J, Morones JR, Camacho-Bragado A, Gao X, Lara HH, Yacaman MJ. Interaction of silver nanoparticles with HIV-1. J Nanobiotechnol. 2005; 3:6.
10. Bhol KC, Alroy J, Schechter PJ. Anti-inflammatory effects of topical nanocrystalline silver cream on allergic contact dermatitis in a guinea pig model. Clin Exp Dermatol. 2004; 29:282–7. [PubMed: 15115512]
11. Takenaka S, Karg E, Roth C, Schultz H, Ziesenis A, Heinzmann U, et al. Pulmonary and systemic distribution of inhaled ultrafine silver particles in rats. Environ Health Perspect. 2001; 109(Suppl 4):547–51. [PubMed: 11544161]
12. Carlson C, Hussain SM, Schrand AM, Braydich-Stolle LK, Hess KL, Jones RL, et al. Unique cellular interaction of silver nanoparticles: size-dependent generation of reactive oxygen species. J Phys Chem B. 2008; 112(43):13608–19. [PubMed: 18831567]
13. Soto K, Garza KM, Murr LE. Cytotoxic effects of aggregated nanomaterials. Acta Biomater. 2007; 3:351–8. [PubMed: 17275430]
14. Sung JH, Ji JH, Yoonn JU, Kim DS, Song MY, Jeong J, et al. Lung function changes in Sprague-Dawley rats after prolonged inhalation exposure to silver nanoparticles. Inhal Toxicol. 2008; 20(6):567–74. [PubMed: 18444009]
15. Hussain SM, Hess KL, Gear hart JM, Geiss KT, Schlarger JJ. In vitro toxicity of nanoparticles in BRL 3A rat liver cells. Toxicol in Vitro. 2005; 19:975–83. [PubMed: 16125895]
16. Arora S, Jain J, Rajwade JM, Paknikar KM. Interactions of silver nanoparticles with primary mouse fibroblasts and liver cells. Toxicol Appl Pharmacol. 2009; 236:310–8. [PubMed: 19269301]
17. Park EJ, Yi J, Kim Y, Choi K, Park K. Silver nanoparticles induce cytoxicity by a Trojan-horse type mechanism. Toxicol in Vitro. 2010; 24:872–8. [PubMed: 19969064]
18. Kawata K, Osawa M, Okabe S. In vitro toxicity of silver nanoparticles at noncytotoxic doses in HepG2 human hepatoma cells. Environ Sci Technol. 2009; 43:6046–51. [PubMed: 19731716]

19. Hussain SM, Javorina AK, Schrand AM, Duhart HM, Ali SF, Schlager JJ. The interaction of manganese nanoparticles with PC-12 cells induces dopamine depletion. Toxicol Sci. 2006; 92(2): 456–63. [PubMed: 16714391]
20. Rosas-Hernandeza H, Jimenez-Badilloa S, Martinez-Cuevasa PP, Gracia-Espino E, Terrones H, Terrones M, et al. Effects of 45-nm silver nanoparticles on coronary endothelial cells and isolated rat aortic rings. Toxicol Lett. 2009; 191(2-3):305–13. [PubMed: 19800954]
21. Braydich-Stolle L, Hussain S, Schlager JJ, Hofmann MC. In vitro cytotoxicity of nanoparticles in mammalian germline stem cells. Toxicol Sci. 2005; 88:412–9. [PubMed: 16014736]
22. Ahamed M, Karns M, Goodson M, Rowe J, Hussain SM, Schlager JJ, Hong Y. DNA damage response to different surface chemistry of silver nanoparticles in mammalian cells. Toxicol Appl Pharmacol. 2008; 233(3):404–10. [PubMed: 18930072]
23. United States Patent USP. 7,135,195. Christensen, RJ. H. “Treatment of humans with colloidal silver composition”. 2006. United States Patent. 6,214,299. Christensen, RJ. H. Apparatus and method for producing antimicrobial silver solution. 2001.
24. Yang J, Wu K, Koňák C, Kopeček J. Dynamic light scattering study of self-assembly of HPMA hybrid graft copolymers. Biomacromolecules. 2008; 9:510–517. [PubMed: 18208316]
25. Tien DC, Tseng KH, Liao CY, Huang JC, Tsung TT. Discovery of ionic silver in silver nanoparticle suspension fabricated by arc discharge method. Journal Alloys, Compounds. 2008; 463(1):408–411.
26. Gibson PG, Wlodarczyk JW, Hensley MJ, Gleeson M, Henley RL, Cripps AW, Clancy RL. Epidemiological association of airway inflammation with asthma symptoms and airway hyperresponiveness in childhood. Am J Respir Crit Care Med. 1998; 158:356–41.
27. Cordray P, Doyle, Edes K, Moos PH, Fitzpatrick FA. Oxidation of 2-cys-perosiredoxins by arachidonic acid peroxide metabolites of lipoxygenases and cycloxygenase-2*. J Biol Chem. 2007; 282(45):32623–9. [PubMed: 17855346]
28. Cameron MD, Aust SD. Degradation of chemicals by reactive radicals produced by cellobiose dehydrogenase from *Phanerochaete chyrsoporium*. Arch Biochem Biophys. 1999; 367(1):115–121. [PubMed: 10375406]
29. Deering-Rice CE, Johansen ME, Roberts JK, Thomas KC, Romero EG, Lee J, et al. Transient receptor potential vanilloid-1 (TRPV1) is a mediator of lung toxicity for coal fly ask particulate material. Mol Pharmacol. 2012; 81(3):411–9. [PubMed: 22155782]
30. Roy S, Basak S, Ray P, Dasgupta AK. Double plasmonic profile of tryptophan–silver nano-crystals - temperature sensing and laser induced antimicrobial activity. Photonics Nanostruct Fund Appl. 2012; 10(4):506–515.
31. Kreibig, U.; Vollmer, M. Optical properties of metal clusters. Vol. Vol 25. Springer; 1995. p. 532
32. Yamamato S, Fujiwara K, Wararai H. Surface-enhanced Raman scattering from oleate-stabilized silver colloids at a liquid/liquid interface. Anal. Sci. 2004; 20:1347–1352. [PubMed: 15478347]
33. Link S, El-Sayed MA. Optical properties and ultrafast dynamics of metallic nanocrystals. Annu. Rev. Phys. Chem. 2003; 54:331–366. [PubMed: 12626731]
34. Angelescu DG, et al. Synthesis and association of Ag(0) nanoparticles in aqueous Pluronic F127 triblock copolymer solutions. Colloids Surf A:. 2011; 394:57–66.
35. Brause R, Moeltgen H, Kleinermanns K. Characterization of laser-ablated and chemically reduced silver colloids in aqueous solution by UV/VIS spectroscopy and STM/SEM microscopy. Appl Phys B: Lasers Optics. 2002; 75:711–716.
36. Lee KS, El-Sayed MA. Gold and silver nanoparticles in sensing and imaging: sensitivity of plasmon response to size, shape, and metal composition. J. Phys. Chem. B. 2006; 110:19220–19225. [PubMed: 17004772]
37. Jin R, Cao Y, Mirkin CA, Kelly KL, Schatz GC, Zheng JG. Photoinduced conversion of silver nanospheres to nanoprisms. Science. 2001; 294:1901–1903. [PubMed: 11729310]
38. Schleh C, Semmler-Behnke M, Lipka J, Wenk A, Hirn S, Schäffler M, et al. Size and surface charge of gold nanoparticles determine absorption across intestinal barriers and accumulation in secondary target organs after oral administration. Nanotoxicology. 2012; 6(1):36–46. [PubMed: 21309618]

39. Panyala NR, Peña-Méndez EM, Havel J. Silver or silver nanoparticles: a hazardous threat to the environment and human health? J Appl Biomed. 2008; 6:117–129.
40. Xia T, Li N, Nel AE. Potential health impact of nanoparticles. Annu Rev Public Health. 2009; 30:137–50. [PubMed: 19705557]
41. Ahamed M, Alsalhi MS, Siddiqui MKJ. Silver nanoparticle applications and human health. Clin. Chim. Acta. 2010; 411:1841–8. [PubMed: 20719239]
42. Nel A, Xia T, Mädler L, Li N. Toxic Potential of Materials at the Nanolevel. Science. 2006; 311:622–7. [PubMed: 16456071]
43. Fischer HC, Chan WCW. Nanotoxicity: the growing need for an *in vivo* study. Curr Opin Biotech. 2007; 18:565–71. [PubMed: 18160274]
44. Greulich C, Kittler S, Epple M, Muhr G, Koller M. Studies on the biocompatibility and the interaction of silver nanoparticles with human mesenchymal stem cells (hMSCs). Langerbecks Arch Surg. 2009; 394:495–502.
45. Lamb JG, Hathaway, Munger MA, Raucy JL, Franklin MR. Nanosilver particle effects on drug metabolism in vitro. Drug Metab Dispos. 2010; 38:2246–51. [PubMed: 20861156]
46. Kim YS, Song MY, Park JD, Song KS, Ryu HR, Chung YH, Chang HK, Lee JH, Oh KH, Kelman BJ, Yu IJ. Subchronic oral toxicity of silver nanoparticles. Part Fibre Toxicol. 2010; 20
47. Xia T, Kovochich M, Brant J, Hotze M, Sempf J, Oberley T, Sioutas C, Yeh JI, Wiesner MR, Nel AE. Comparison of the abilities of ambient and manufactured nanoparticles to induce cellular toxicity according to an oxidative stress paradigm. Nano Lett. 2006; 8:1795–1807.
48. Jun E-A, Lim K-M, Kim K, Bae ON, Noh JY, Chung KH, et al. Silver nanoparticles enhance thrombus formation through increased platelet aggregation and procoagulant activity. Nanotoxicol. 2011; 5(2):157–67.
49. O'Hagan DT. The intestinal uptake of particles and implications for drug and antigen delivery. J Anal. 1996; 189:477–82.

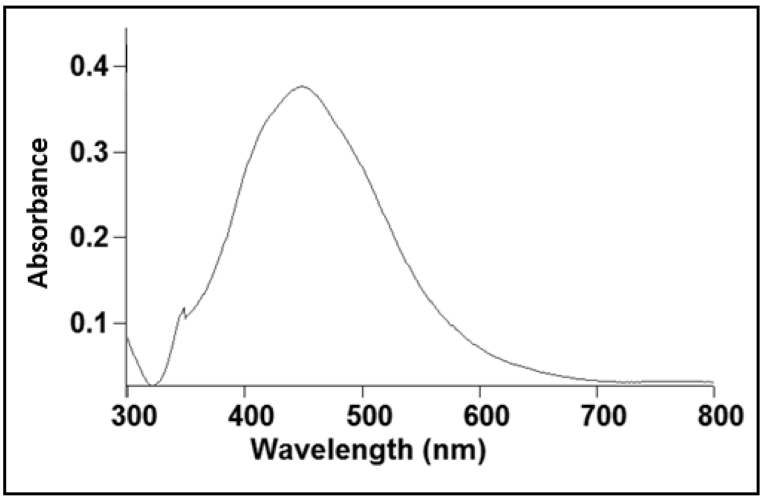

Figure 1.
Optical absorbance spectrum of 32ppm commercial AgNPs measured on samples taken directly from the study stock bottle used in human oral ingestion and exposures (lot # 09280).

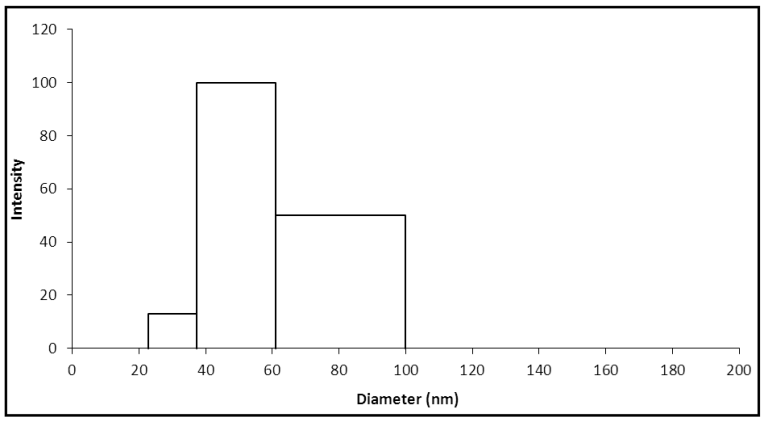

Figure 2.
Dynamic Light Scattering (DLS) particle size characterization of 32 ppm commercial AgNPs as taken directly from commercial silver nanoparticle sample (lot # 09280).

Table 1

Study Population Demographics

Demographic/Clinical Variable	10 ppm (n=36)	32 ppm (n=25)	Total Sample (n=61)
Age, years, mean±SD min, max	52±11 26-76	41±15 20-67	47±14 20-76
Gender, n M/F (%)	17/19 (47/53)	18/6 (75/25)	35/25 (58/42)
BMI (kg/m2) mean±SD (min, max)	29±6 20-45	29±6 21-43	29±6 20-45
SBP (mmHg) mean±SD (min, max)	127±19 84-176	127±13 102-150	127±17 84-176
DBP (mmHg) mean±SD (min, max)	83±11 55-106	81±11 62-107	82±11 55-107
Heart Rate (bpm) mean±SD (min, max)	69±9 42-84	65±7 52-79	68±8 42-84

Table 2

Study Population Changes in Hemodynamics

Hemodynamic Variable	10 ppm Mean Change [95% CI] (*p* value)	32 ppm Mean Change [95% CI] (*p* value)	Total Sample Mean Change [95% CI] (*p* value)
Weight (kg)	−1.1[−2.6, 0.4] (0.17)	−0.4[−0.1, 0.8] (0.13)	−0.5[−1.4, 0.4] (0.30)
BMI (kg/m^2)	−0.4[−0.9, 0.1] (0.15)	−0.1[−0.04, 0.3] (0.14)	−0.2 [−0.5, 0.1] (0.26)
SBP (mmHg)	1.3[−1.7, 4.3] (0.40)	−1.3[−3.0, 5.6] (0.54)	1.3[−1.2, 3.8] (0.30)
DBP (mmHg)	−2.4[−5.5, 0.7] (0.13)	−0.7[−2.5, 3.8] (0.67)	−1.2 [−3.4, 1.1] (0.31)
HR (bpm)	−1.9[−5.0, 1.3] (0.25)	−3.1[−6.4, 0.3] (0.07)	−2.3 [−4.6, −0.93] (0.05)

BMI: Body Mass Index; SBP: Systolic blood pressure; DBP: Diastolic Blood Pressure; HR: Heart Rate; CI; Confidence Interval

Table 3

Study Population Comprehensive Metabolic Panel and Complete Blood Count with Differential (10 ppm [n=36], 32 ppm [n=24], Total Sample [n=60])

Comprehensive Metabolic Panel and Complete Blood Cell Count with Differential	10 ppm Mean Change [95% CI: min, max] (*p* value)	32 ppm Mean Change [95% CI: min, max] (*p* value)	Total Sample Mean Change [95% CI: min, max] (*p* value)
Sodium [mmol/L]	−0.1[−0.7, 0.6] (0.87)	0.2 [−0.7, 1.0] (0.71)	0.03 [−0.5, 0.6] (0.90)
Potassium [mmol/L]	−0.1[−0.3, 0.02] (0.10)	−0.03 [−0.2, 0.1] (0.74)	−0.08 [−0.2, 0.03] (0.13)
Chloride [mmol/L]	−0.4[−1.2, 0.3] (0.23)	0.04[−1.1, 1.2] (0.94)	−0.3[−0.9, 0.4] (0.44)
Carbon Dioxide [mmol/L]	0.5[−0.5, 1.6] (0.33)	−0.04[−1.1, 1.0] (0.94)	0.3[−0.5, 1.1] (0.44)
BUN* [mg/dL]	−0.9[−1.7, −0.1] (0.03)**	0.5 [−0.08, 1.8] (0.41)	−0.3 [−1.1, 0.4] (0.37)
Creatinine [mg/dL]	0.01 [−0.02, 0.03] (0.60)	−0.02 [−0.04, 0.01] (0.21)	−0.003 [−0.02, 0.01] (0.74)
Glucose [mg/dL]	3.6 [−1.6, 8.7] (0.17)	−0.7 [−4.2, 2.9] (0.71)	1.9 [−1.5, 5.3] (0.28)
ALP [U/L]	−1.4 [−3.9, 1.1] (0.28)	2.0 [−1.0, 5.0] (0.18)	−0.03 [−2.0, 1.9] (0.97)
AST [U/L]	−0.44 [−2.1, 1.2] (0.60)	2.0 [−2.6, 6.5] (0.40)	0.5 [−1.5, 2.5] (0.61)
ALT [U/L]	−2.6 [−4.8, −0.3] (0.03)**	2.3 (−1.6, 6.3) (0.25)	−0.6 (−2.7, 1.5) (0.58)
Total Protein [g/dL]	−0.02 [−0.3, 0.2] (0.87)	0.2 [−0.001, 0.4] (0.051)	0.1 [−0.1, 0.3] (0.45)
Total Bilirubin [mg/dL]	−0.02 [−0.08, 0.3] (0.43)	−0.03 [−0.11, 0.05] (0.49)	−0.02 [−0.07, 0.02] (0.29)
Albumin [g/dL]	−0.07 [−0.1, 0.0004) (0.06)	0.11 [−0.01, 0.23] (0.09)	0.002 [−0.07, 0.07] (0.96)
Calcium [mg/dL]	−0.1 [−0.2, 0.04] (0.20)	0.1 [−0.003, 0.2] (0.06)	0.0 [−0.1, 0.1] (0.99)
WBC Count [k/μL]	−0.17 [−0.53, 0.19] (0.35)	−0.09 [−0.68, 0.49] (0.75)	−0.14 [−0.46, 0.17] (0.38)
RBC Count [M/μL]	−0.08 [−0.17, −0.001] (0.047)**	0.06 [−0.03, 0.14] (0.23)	−0.03 [−0.09, 0.03] (0.37)
Hemoglobin [gm/dL]	−0.2 [−0.4, 0.03] (0.08)	0.1 [−0.2, 0.4] (0.41)	−0.1 [−0.3, 0.1] (0.41)
Hematocrit [%]	−0.7 [−1.5, 0.07] (0.075)	0.8 [−0.1, 1.7] (0.095)	−0.1 [−0.8, 0.5] (0.68)
MCV [fL]	0.1 [−0.6, 0.8] (0.80)	0.5 [−0.1, 1.2] (0.12)	0.3 [−0.2, 0.7] (0.29)
MCH [pg]	0.1 [−0.1, 0.3] (0.48)	−0.1 [−0.4, 0.2] (0.38)	−0.01 [−0.2, 0.2] (0.96)
MCHC [gm/dL]	0.1 [−0.3, 0.4] (0.72)	−0.3 [−0.7, 0.1] (0.12)	−0.1 [−0.3, 0.2] (0.53)
Platelets [k/μL]	5 [−6, 15] (0.39)	−4 [−16, 8] (0.53)	1.3 [−6.8, 9.4] (0.76)
Granulocytes [%]	−0.9 [−3.0, 1.1] (0.36)	−0.7 [−4.0, 2.7] (0.70)	−0.9 [−2.8, 1.0] (0.36)
Lymphocytes [%]	0.7 [−1.2, 2.6] (0.46)	1.3 [−1.5, 4.1] (0.36)	1.0 [−0.8, 2.7] (0.27)
Monocytes [%]	−0.1 [−0.6, 0.4] (0.70)	−0.3 [−0.8, 0.3] (0.34)	−0.2 [−0.5, 0.2] (0.38)
Basophils [%]	0.04 [−0.1, 0.2] (0.58)	0.001 [−0.1, 0.1] (0.99)	−0.02 [−0.1, 0.1] (0.61)
Eosinophils [%]	−0.06 [−0.3, 0.2] (0.69)	−0.2 [−0.7, 0.2] (0.36)	−0.1 [−0.4, 0.1] (0.35)

* BUN- Blood Urea Nitrogen; ALP: Alkaline Phosphatase; AST: Aspartate Aminotransferase; ALT: Alanine Aminotransferase; WBC: White Blood Cells; RBC: Red Blood Cells; MCV: Mean Corpuscular Volume; MCH: Mean Corpuscular Hemoglobin; MCHC: Mean Corpuscular Hemoglobin Concentration.

** $p \leq 0.05$ Comparison of 10 ppm or 32 ppm active solution vs. placebo solution, controlling for baseline value, in a mixed effects linear regression model.

Table 4

Sputum Reactive Oxygen Species and Pro-inflammatory Cytokine Analyses

ROS or Cytokine Parameter	10 ppm Mean Change [95% CI] (*p* value)	32 ppm Mean Change [95% CI] (*p* value)	Total Sample Mean Change [95% CI] (*p* value)
ROS μM	0.89 [−0.6, 2.38] (0.24)	−0.44 [−1.23, 0.35] (0.28)	0.52 [−0.56, 1.60] (0.34)
IL-8 (copies/1000 B2M)*	2.19 [−1.53, 5.91] (0.25)	6.39 [−5.83, 18.60] (0.31)	4.52 [−2.47, 11.51] (0.21)
IL-1α (copies/1000 B2M)	−0.0005 [−0.0007, 0.0006] (0.88)	0.0197 [−0.0014, 0.0408] (0.07)	0.0128 [−0.0014, 0.0269] (0.08)
IL-1β (copies/1000 B2M)	0.017 [−0.011, 0.044] (0.24)	0.027 [−0.058, 0.112] (0.53)	0.022 [−0.027, 0.072] (0.38)
MCP1 (copies/1000 B2M)	−0.028 [−0.084, 0.028] (0.34)	−0.004 [−0.026, 0.017] (0.69)	−0.015 [−0.046, 0.015] (0.33)
NQO1 (copies/1000 B2M)	−0.0043 [−0.0115, 0.029] (0.24)	−0.0279 [−0.4671, 0.4114) (0.90)	−0.0182 [−0.2850, 0.2487] (0.89)

ROS: Reactive Oxygen Species; B2M: Beta-2 microglobulin; MCP1: Monocyte chemoattractant protein-1; NQO1: NADH quinine oxioreducatase-1